

On the Temperature Acclimation of
Crustacea Musculature:
A Comparison of Warm and Cold Muscle
Responses in the Crab,
Cancer borealis

A Senior Honors Thesis

Presented to:
The Faculty of the Undergraduate School of Arts and Sciences
Brandeis University
Neuroscience Department
Dr. Eve Marder, Advisor

In Partial Fulfillment of the Requirements for
Graduation with Honors

Jonathan Theodore Smith
December 2007

Table of Contents

Table of Contents1
Abstract2
Introduction3-5
Materials and Methods6-13
Results14-18
Discussion19-22
Conclusion23
Acknowledgements24
References25
Figures26-40

Abstract

Temperature is a universal variable that impacts the lives of every living creature on this planet. Without proper temperature constraints, life wouldn't be possible (at least as we know it). Creatures must interact and cope with their environments and adapt to environmental variables such as temperature.

Recent findings suggest that long term temperature acclimation changes the output of the stomatogastric ganglion (STG), a central pattern generator in the stomach of decapod crustacea. The neurons of the STG control the stomach contractions required for digestion of food.

Given that the neurons in the STG undergo long-term changes when acclimated to a particular temperature, this study investigated the changes in muscles in response to temperature acclimation. These changes were assayed using a modeling technique developed and tested on other muscles in the foregut of the crab, *Cancer borealis*.

Two populations of temperature acclimated crabs were used: 19°C and 7°C acclimated crabs. The responses elicited by stimulation of the p1 muscle showed significant changes across both acute and acclimation temperatures. The maximum amplitude of p1 muscle responses in 7°C acclimated crabs was significantly higher than in some 19°C acclimated animals. The falling time constant for the responses was significantly lower in 7°C acclimated crabs when compared with the warmer acclimated animals. The facilitation of these synapses was not significantly affected.

These results suggest that properties of the muscles themselves are changing, whereas properties of the presynaptic terminal are unaffected by temperature acclimation.

Introduction

The world in which we live is a complex system – every factor of our environment, including other people and animals, can and does change how we act. One of the most important factors for life is thermal energy, temperature. For homeothermic animals, such as humans, the immediate temperature of the surrounding environment, while it does to some degree affect the body, will not dictate the internal temperature of the organism. Such animals do not need to drastically compensate for environmental temperature fluctuations, save for, perhaps, maintaining an insulating layer of blubber (seals), or even throwing on a sweater (humans). For ectotherms, the problem is considerably more important and complex – with no way to internally regulate their temperature, they must find some way to perform at whatever temperature they encounter, or die trying.

Many experiments have investigated how animals respond to temperature perturbations. In the copepod, *Calanus finmarchius*, many aspects of the escape response vary reliably with temperature (Lenz et al., 2005). The resting potential of muscle fibers in the crab (*Carcinus maenas*), the cockroach (*Periplanta americana*), and the frog (*Rana temporaria*), have been shown to increase as temperature decreases (Kerkut and Ridge, 1960). The heart rate in the lobster, *Homarus americanus*, increases (up to $T = 14^{\circ}\text{C}$) then decreases (after $T = 14^{\circ}\text{C}$) with temperature increase (Worden et al., 2006).

The crab, *Cancer borealis*, aside from being meaty and delicious, is a good model organism in which to study temperature effects. The stomatogastric ganglion (STG) provides coordinated control to the musculature of the stomach of decapod crustacea. The network of axons projecting from the STG, the stomatogastric nervous system

(STNS), is one of the best understood neural networks. One particular output of the STG is the pyloric rhythm, which mediates control of the filtering of food in the crab stomach. This pyloric rhythm is generated by the anterior burster (AB) neuron and the two electrically coupled pyloric dilator (PD) neurons, which act as the pacemaker of the rhythm (Hooper et al., 1986). These cells send inhibitory processes to the lateral pyloric (LP) and the five pyloric neurons (PY). It is the interactions of these neurons result in the triphasic pyloric rhythm.

Recently, the pyloric rhythm has been shown to increase as a function of acute temperature increase (Figure 1) (L.S. Tang, personal communication). A related study has also indicated that acclimating crabs at different temperatures for extended periods of time changes the resilience of the pyloric rhythm at higher temperatures, and results in breakdowns of the network at different temperatures (L.S. Tang, personal communication). The differences of breakdown temperature threshold indicate that there is some homeostatic compensation for long-term temperature exposure in the STNS. Acclimation was found to change cardiac performance in *Homarus americanus* - overall heart rate is increased in 4°C acclimated animals (Camacho et al., 2006). Above 20°C breakdowns (similar to pyloric rhythm breakdowns, i.e. heart failure) were also seen (Camacho et al., 2006). Clearly some homeostatic changes take place during temperature acclimation on stomatogastric and cardiac performance.

While it is known that the neuromuscular junctions of the muscles innervated by the STG are modulated by various substances (Jorge-Rivera et al., 1998), it was unclear whether there was some change in these muscles as a response to temperature acclimation. Do stomach muscles in the crab cease to function at high temperatures? Do

muscles compensate for changes in temperature in addition to the network? In this study, I investigated these questions.

The pyloric muscle (p1) is innervated by the lateral pyloric (LP) neuron via the lateral ventricular nerve (*lvn*). Artificial stimuli were applied to P1 by stimulating the LVN, and a profile of muscle responses was determined at many acute temperatures in animals acclimated to different temperatures.

To assess for changes in muscle function, rather than delivering paired pulse stimulation, measuring the maximum voltage of excitatory junctional potentials (EJPs), and calculating a simple facilitation index, a modeling approach was taken. The model proposed by Sen et al. (1996) provides for changes in not only gross muscle response but also in facilitation, and can be more fine-grained than a somewhat gross analysis of EJP height alone. The model has been tested on data from muscles within the stomach of *Cancer borealis* crabs, and was shown to accurately predict their responses. This model was fit to the data recorded from the two populations of temperature acclimated crabs and then differences in each model were compared.

Materials and Methods

Animals

All animals were adult *Cancer borealis* crabs and were bought from local fishermen (Commercial Lobster). Animals were acclimated to either 7°C or 19°C in artificial seawater for at least two weeks without food until used.

Muscle Preparation

Crabs were anesthetized on ice for at least 30 minutes prior to dissection. First the stomach was removed, then the p1 muscle and lateral ventricular nerve (*lvn*) were identified following the nomenclature of Maynard and Dando (1974), and dissected out. The muscle preparation was then pinned out in a 60 mm X 15 mm plastic Petri dish (Fisher Scientific) with the LVN still attached. Dishes were coated in Sylgard (Dow Corning).

Saline

All preparations were immersed in saline consisting of the following: Millipore filtered water containing (in mM) 440 NaCl, 26 MgCl₂ · 6H₂O, 13 CaCl₂ · 2H₂O, 11 KCl, 12 trizma base, 5 maleic acid. Saline was buffered to a pH of 7.4-7.5. During recording, saline was superfused across the muscle preparation at an average flow rate of 5 ml/min using a gravity feed system.

Electrophysiology

Stimulation

A Vaseline well was constructed around the *lvn*, and a stainless steel extracellular electrode was used to stimulate the *lvn*. The electrode was connected to a differential amplifier (A-M Systems, model 1700), which, in turn, was connected to an isolated pulse

stimulator (A-M Systems, model 2100). The individual stimuli were created by sending a TTL signal to the stimulator. The individual stimulations lasted 0.5 ms and were at an average voltage of 2 V.

There were three distinct types of stimulus trains. A first Poisson stimulus set consisted of 1 Hz and 2 Hz Poisson trains, with absolute refractory periods of 500 ms each. A second stimulus set consisted of stimulus trains extracted from traces of a lateral pyloric (LP) neuron at increasing acute temperature (7°C, 11°C, 19°C, 27°C, 31°C). The third set of stimuli was another set of Poisson trains at 5 Hz, 10 Hz, and two at 20 Hz. The absolute refractory period for each of these was 50 ms, 50 ms, 100 ms, and 50 ms, respectively. Each stimulus train was administered at each acute temperature resulting in five presentations of each stimulus train per preparation. After reaching 31°C, three of the 19°C acclimated crabs and three of the 7°C acclimated crabs were brought back down to 7°C and stimulated again as a control.

Recording

Intracellular electrodes were used to record excitatory junctional potentials (EJPs) and measured input resistance in the p1 muscle. The electrodes were pulled using a Flaming/Brown micropipette puller (Sutter Instruments, model P-97) from borosilicate glass micropipettes with filaments (Sutter Instruments, item# BF100-78-10). Electrodes were filled with a salt solution consisting of 0.6 M K₂SO₄, 20 mM KCl. Electrodes had a resistance of 15-10 MΩ.

Input resistance was measured by injecting 1 nA of current into the muscle fiber and recording the voltage deflection. The voltage deflection was averaged over multiple

current injections at each temperature. The difference in voltage corresponded to some discrete input resistance value as given by Ohm's law ($V = IR$).

Electrodes were connected to a 1x gain headstage running to an Axoclamp-2A (Axon Instruments). The Axoclamp was connected to an instrumentation amplifier (Brownlee Precision, model 440), then to a Digidata 1322A electronic data acquisition system (Axon Instruments) connected to a computer. Data were sampled at 5 kHz using Clampex (ver. 9.0.2.18) software (Axon Instruments).

Bath volume during recording was on average 4 ml. During each trial, saline was maintained at the appropriate temperatures using a peltier cooling system (Warner Instruments, model CL-100).

Model Analysis

All data were analyzed using Spike2 software (Cambridge Electronic Design, ver. 6.04), and Matlab (The Mathworks, ver. 7.4.0.287).

Model

In order to characterize the electrical responses of the muscle, a modeling technique was employed. A synaptic decoding model characterized by Sen. et al. (1996) was implemented in Matlab, with some modifications. The model is based on the fitting of three functions, K_1 , K_2 , and F . These three functions are the kernel of a single spike response, the kernel of the facilitation, and the scaling of facilitation (to allow for nonlinear facilitation), respectively.

Given a single spike at time t_i , the response of the muscle is given by the equation $K_1(t - t_i)$. For an arbitrary train of stimuli, the estimated response of the muscle at a given time, t , ($R_{est}(t)$) is given by equations 1 through 3:

$$R_{est}(t) = \sum_{t_i < t} K_1(t - t_i) [1 + A(t_i)] \quad (1)$$

$$A(t_i) = F(S(t_i)) \quad (2)$$

$$S(t_i) = \sum_{t_j < t_i} K_2(t - t_i) \quad (3)$$

As in Sen et al., K_1 was determined by fitting a function to an average of single responses. These single responses were averaged from the Poisson stimulus trains of 1 Hz and 2 Hz with 500 ms refractory periods. At higher temperatures multiple spikes were elicited from each single stimulus. For these responses, data up to the visible threshold of the second EJP were averaged together, ignoring all data after the onset of this second response. Unlike Sen et al., an alpha function was chosen to represent K_1 because it allows for a nonlinear rise as well as an exponential decay, which more closely resembles single EJP recordings. The particular alpha function used is a modified version of one found in Dayan and Abbott (2001), and is shown in equations 4 through 6.

$$K_1(t - t_i) = \alpha(t_{tot}) = V_{max} \cdot B \cdot \left(\exp\left(\frac{-(t_{tot} - t_{shift})}{\tau_1}\right) - \exp\left(\frac{-(t_{tot} - t_{shift})}{\tau_2}\right) \right) \quad (4)$$

$$B = \left(\left(\frac{\tau_1}{\tau_2} \right)^{(\tau_{rise}/\tau_1)} - \left(\frac{\tau_2}{\tau_1} \right)^{(\tau_{rise}/\tau_2)} \right)^{-1} \quad (5)$$

$$\tau_{rise} = \frac{\tau_1 \tau_2}{\tau_1 - \tau_2} \quad (6)$$

With 2 conditions:

$$\tau_1 > \tau_2$$

$$\text{if } K_1 < 0, K_1 = 0$$

The time to the peak of the alpha function from $t_{tot} - t_{shift} = 0$ can be derived using the above equations as:

$$time\ to\ peak = \tau_{rise} \ln\left(\frac{\tau_1}{\tau_2}\right) \quad (7)$$

Fitting the K_2 and F functions required an iterative minimization algorithm. One of the algorithms used was a quasi-Newtonian minimization as implemented by the Matlab function *fmincon*. The other was a Powell's method (A. L. Taylor, personal communication) which had already been implemented in Matlab.

The function to be minimized and trained upon was an error function calculated on each sample point of the raw data and the corresponding sample in the model's estimate. The error at each sample was then averaged together to get the average error for a particular stimulus train. The stimulus train data was then averaged together to form an overall average error for training. The response functions in this error calculation then become functions of a sampling point index, rather than functions of time:

$$TrainingError = \frac{1}{n} \sum_{j=1}^n \left[\frac{1}{T} \int_0^T (R_{exp(j)}(t) - R_{est(j)}(t))^2 dt \right] \quad (8)$$

Where:

n = number of Poisson stimulus trains given

T = number of samples in a given data train

R_{exp} = expected response from the muscle (experimental data)

Stimulus training data consisted of four Poisson stimulus trains – 20 Hz, 20 Hz, 10 Hz and 5 Hz. All trains had a refractory period of 50 ms except one 20 Hz, which used 100 ms. These times were chosen by looking at the natural interspike intervals (ISIs) within the bursts of LP trains at varying temperature – 50 ms was the smallest ISI reliably found.

The parametric forms for both K_2 and F were created by first assuming nothing about the parametric representations and instead using a discrete set of values for each time bin. By fitting the values of K_2 and F at time bins, a functional form emerged

without requiring prior assumptions and thereby limiting the accuracy of the model. These initial discrete approximations of K_2 and F were calculated using *fmincon*. All other minimizations were performed by the Powell method.

The K_2 discrete response resembled an alpha function, as opposed to an exponential decay as in Sen et al. (1996). The alpha function was tested against an exponential K_2 fit for two randomly sampled data points. In both cases, the alpha function produced slightly lower testing error than the exponential decay. The alpha function formula chosen was the same as that chosen for K_1 (equations 4-7), with one exception - t_{shift} was set to be 0 for all K_2 functions. The rationale behind this choice was that there was no available evidence to suggest that facilitation was absolutely delayed by a period of time before acting. The parameters of this K_2 function were then refined using the minimization algorithm, assuming F was the identity function.

The F function was then parameterized in a similar fashion to K_2 . Notably, K_2 was not allowed to vary while the discrete form of F was determined. The parameterized equation ultimately chosen was the same as in Sen et al.:

$$F(x) = Ax^2 + Bx \quad (9)$$

Once parameterized forms of F and K_2 were determined, an arbitrary starting point was chosen for both and they were minimized together.

To assess the accuracy of the model, a dataset consisting of 5 LP spike trains from several acute temperatures (7°C, 11°C, 19°C, 27°C, 31°C) given to each muscle preparation at each acute temperature (7°C, 11°C, 19°C, 27°C, 31°C) was used. The stimulus times from all of the 5 LP trains were given to the model for each animal at each acute temperature. The results of these models were compared to the corresponding

experimental data using a relative root mean squared (RMS) error assessment. This error was calculated on each sample point in the following fashion:

$$TestingError = 100 \cdot \sqrt{\frac{1}{n} \sum_{j=1}^n \left[\left(\frac{RMSE_j}{RMSA_j} \right)^2 \right]} \quad (10)$$

where:

$$RMSE_j = \sqrt{\frac{1}{m} \sum_{i=1}^m \left[\left(R_{\text{exp}}^j(i) - R_{\text{est}}^j(i) \right)^2 \right]} \quad (11)$$

$$RMSA_j = \sqrt{\frac{1}{m} \sum_{i=1}^m \left[\left(R_{\text{exp}}^j(i) \right)^2 \right]} \quad (12)$$

and:

n = number of LP stimulus trains given
m = number of samples in a given data train
 $R_{\text{exp}}^j(t)$ = experimental data on the jth stimulus

To summarize formulas 10-12, the relative RMS error was computed for each given LP stimulus train in a point-wise fashion (on each data sample). These relative RMS errors were squared, then averaged across all LP trains. The square root was then taken and the result was multiplied by 100 to get a percentage.

A model, consisting of idealized K_1 , K_2 , and F parameters, was created for each animal at each acute temperature, resulting in a total of 40 models – 20 for 7°C acclimated animals, 20 for 19°C acclimated animals. To save computation time, the training and testing data were downsampled by a factor of 2 to an effective sampling rate of 2.5 KHz.

For higher acute temperatures ($T \geq 19^\circ\text{C}$), a single stimulus often produced multiple EJPs (presumably due to generation of additional spikes in the *hvn*). For these,

spike times were approximated by finding the time of the peaks in the EJPs and subtracting the time to peak and the t_{shift} parameter in the K_1 kernel.

After fitting the model to all animals at every temperature, it was immediately clear that one 7°C acclimated animal, and one 19°C acclimated animal were qualitatively different from the other animal models across all acute temperatures. Moreover, they gave different responses at 7°C at different times. These two animals were discarded for the purposes of statistical analysis.

Statistical Analysis

All tests for statistical significance were performed using SigmaStat software (Systat Software Inc., ver. 3.5.0.54). Tests included t-tests, paired t-tests, 2-way repeated measures ANOVA, repeated measures ANOVA on ranks.

Results

In order to measure the temperature-dependence of the electrical response of the p1 muscle, preparations were dissected out of acclimated (to either 7°C or 19°C) animals and recorded from at five acute temperatures (7°C, 11°C, 19°C, 27°C, 31°C). Several stimulus trains were administered at each temperature and a model was fit to the collected data.

In an effort to extract biologically-relevant information, neuronal activity trains were chosen from an LP neuron at each of the five acute temperatures. These data, because of their biological significance (i.e. they are actual LP stimulus trains), were used to assess the accuracy of the model. These LP stimulus trains were given to each muscle preparation via extracellular stimulation of the *l_{vn}* (Figure 2, Figure 3). There is a notable decrease in EJP amplitude with increasing acute temperature.

To determine the basic shape of a single EJP, slow Poisson stimulus trains (1Hz and 2Hz, 500ms minimum ISI) were given to each preparation at each temperature. Examples of typical EJPs in response to single stimuli at varying temperature are in Figures 4 and 5. The marked decrease in maximum EJP amplitude with increasing temperature is apparent in these single stimuli. Additionally, the time from stimulus to EJP threshold seems to shorten.

The model was fit to Poisson trains in each preparation at each acute temperature. Figures 6 and 7 show examples of the same 10Hz Poisson train given to a 7°C and a 19°C acclimated crab at increasing acute temperatures respectively. As a control, model parameters were compared at the initial 7°C and on the return to 7°C after reaching 31°C. There were no significant differences between these data (paired t-tests, $p > 0.1$).

However, the test was below the recommended power level (0.8), so there may have been significant differences that were undetected.

Does the shoe fit? – The fit of the model

Figure 8A shows the results of fitting the model to a 7°C acclimated p1 muscle at an acute temperature of 11°C, given a 7°C LP stimulus train as testing data. Figures 8B-D show the plot of the K_1 kernel, the K_2 kernel and the F function respectively. Figure 9A shows the results of fitting the model to a 19°C acclimated p1 muscle at an acute temperature of 11°C, using a 7°C LP stimulus train as testing data. The model was able to reproduce some subtle features of each stimulus train. The single spike depression seen within a single burst is not entirely expected, yet the model depresses at those stimuli. This is a good indication that the model itself is effective at predicting the muscle response to an arbitrary train of stimuli. The average testing error for each animal overall was $37.43 \pm 2.9\%$ (standard error of the mean); minimum was 19.31%, maximum was 69.48%. The errors of the models are somewhat higher than those produced by Sen et al (1996). However, this is likely due to the error metrics used in these fits, and is not necessarily indicative of bad fitting.

Figure 10 shows the K_1 kernels for every animal at every acute temperature. This layout allows for a visual assessment of the changes across temperature and between acclimations. Rather than average the model parameters within each acclimation temperature, each individual fit of the model was kept for each animal and used in analysis. This was done because it was unclear that averaging within acute temperatures would result in meaningful data – the resulting model may not have fit any of the individual traces well, due to interanimal variability.

Figure 11 shows the K2 kernels for every animal for 7°C, 11°C and 19°C. Figure 12 shows the F functions for all animals at the same temperatures. Unexpected experimental results prevented straightforward analysis of higher acute temperature data (27°C and 31°C) (explained below).

Single EJP Max Amplitude Changes Significantly Across Acute Temperatures and Acclimation Temperatures

A two way repeated measures ANOVA was performed on parameters of the K1 kernel for each animal at both acclimation temperatures. Figure 13A shows the values for V_{max} , the maximum single EJP amplitude as fit by the model. The markers above data points show significant differences. Interestingly, there was a significant effect of acclimation temperature, but only within the data at an acute temperature of 7°C ($P < 0.05$). There also was a significant effect of acute temperature on V_{max} in the 7°C acclimated animals ($P < 0.005$), but not in 19°C acclimated animals ($P > 0.02$).

The Falling Time Constant of a Single EJP Changes Significantly Across Acute Temperatures and Acclimation Temperatures

Another two way repeated measures ANOVA was performed, this time on τ_{1} , the falling time constant of a single EJP. Figure 13B shows the final parameter values of τ_{1} for all animals. The markers above data points show significance. There was a significant difference between acclimation temperatures in τ_{1} in acute temperatures 7°C and 11°C ($P < 0.05$). Additionally, there was a significant effect of acute temperature within the 7°C acclimated animals ($P < 0.005$). A similar acute temperature effect was seen on τ_{1} in the 19°C acclimated animals ($P < 0.005$).

The Time from Stimulus to Threshold of a Single EJP changes Significantly with Acute and Acclimation Temperature

Figure 13C shows the final parameter values of t_{shft} , the time from stimulus to threshold in a single EJP. Yet another two way repeated measures ANOVA was

performed on this data. The markers above data points show significance. There was a statistically significant difference between acute temperatures within 7°C acclimated animals ($P < 0.005$). Additionally, there was a statistically significant difference between acute temperatures within 19°C acclimated animals ($P < 0.01$). A statistically significant difference was found between acclimation temperatures within the 31°C parameters ($P < 0.05$).

Facilitation Does not Differ Significantly with Acute or Acclimation Temperatures

A two way repeated measures ANOVA was performed on max and tau_1 of K2 across all animals, and on the quadratic and linear coefficients (A , B) of the F functions across all animals in acute temperatures of 7°C, 11°C and 19°C. No significant differences were found. A repeated measures ANOVA on ranks was performed on the K2 time to peak data for each acclimation temperature. Additionally a t-test was performed on time to peak data between acclimation temperatures for 7°C acute temperature data. Again, no significant effects of temperature of any kind were reported. Figures 14A and 14B show the max parameter for K2 and the linear coefficient for F respectively across all animals from acute temperatures 7°C – 19°C. The significance tests reported a low power, which could have led to no significant findings.

Input Resistance Changes as a function of Acute Temperature in 7°C acclimated animals

Figure 14C shows the input resistance measurements of all animals in all acute temperatures. The markers above data points show significance. A t-test was run to determine significant differences between acclimation temperatures – none were found. A repeated measures ANOVA on ranks was performed on both the 7°C and 19°C acclimated input resistance data. Significant differences were found only within the 7°C

acclimated input resistances ($P < 0.005$). Despite a significant effect of acute temperature, the input resistances are for the most part rather stable, indicating good recording quality. Moreover, the changes in input resistance are not very large across acute temperatures.

Single Stimuli Elicit Multiple EJP Responses at High Temperatures

The unexpected results that were immediately apparent were that when animals were raised to the higher acute temperatures, a single stimulus would elicit multiple EJPs from the muscle. This phenomenon is illustrated in Figure 15. The effect seemed to begin at lower temperatures in 19°C animals, but was present in most cases once temperature reached and exceeded 27°C. The multiple responses seemed to be caused by repeated spikes of the motor axon in response to a single stimulus. This phenomenon has been reported at high temperatures for the innervating axons of crustacean musculature in the past (Stephens and Lazarus, 1981; Stephens and Atwood, 1981; Stephens, 1985, Stephens and Atwood, 1982; Lazarus et al., 1982). As seen in Figure 15, the additional spikes clearly cause appreciable facilitation. Without knowing the stimulus times, analysis using this method would be difficult at best, for an inaccurate picture of facilitation would emerge, potentially confounding the rest of the model. For all such multiple spikes at 19°C acute temperature, the stimulus times were approximated by subtracting time to peak and t_{shift} as determined in the K1 parameters for a given animal. Multiple responses at higher temperatures were not analyzed.

Discussion

The data above clearly show that there are compensatory mechanisms in the p1 muscle due to prolonged temperature exposure. Ocean temperature is inherently variable from season to season, so this is not entirely unexpected for a marine animal. The crashes seen in the STG at high temperatures do not manifest themselves as such in the muscles. The analogous effect is likely due, instead, to increased activity not in the muscles themselves, but generated in the axons that innervate them.

The analysis of these data using this particular model provides some very interesting insights. Analyzing only EJP amplitude, the facilitation would be apparent, but probable causes would be less easy to separate. In terms of the biological equivalence to the model, the K_1 kernel could correspond to the post-synaptic muscle fiber, and how it responds to activation from the nerve. K_2 and F are both measures dealing with facilitation, presumably in the pre-synaptic terminal. Sen et al. (1996) suggested the possible biological significance of these two functions: the K_2 kernel could represent pre-synaptic calcium flux and the F function could represent the relationship of transmitter release to calcium concentration within the pre-synaptic terminal.

Given that the pyloric frequency increases as acute temperature rises (L. S. Tang, personal communication), my expectation would be a lower maximum EJP amplitude to result in the same net activation of the muscle. This is demonstrated fairly well at least in the 7°C acclimated animals (Figure 13A), and these results correspond with what has been found in other studies for EJP maximum amplitude in crustacean muscles with acute temperature increase (Stephens and Atwood, 1981). Acclimated animals should therefore exhibit lower maximum EJP amplitude across all temperatures, if they have compensated

for high temperatures on a longer time scale. This is partly shown in Figure 13A between 7°C acclimated animals and 19°C acclimated animals at an acute temperature of 7°C.

The expectations of the time course of the muscle response are somewhat less intuitive. As acute temperature increases, the decay time of the EJP decreases (Figure 13B). This has been found in the bender muscle fibers in *Ocypode ceratophthalma*, the Hawaiian ghost crab, as well (Stephens, 1985). This would also lead to having a lesser effect in the muscle, because the voltage deflection from baseline for a single response would be over more quickly and would be less likely to overlap with another EJP. From a physical standpoint, these expectations make sense – things tend to speed up with increasing acute temperature. The overall larger time constants in 19°C acclimated animals when compared with 7°C acclimated animals (at least for 7 and 11°C acute temperature) seems to jibe with this hypothesis. Given that the 19°C acclimated animals would have to adapt to having consistently shorter (in duration) EJPs, the channel densities would likely change to cause the EJPs to either rise more slowly or decay more slowly. A decreased rise time may not be desirable, however, as that would lead to a delay in reaction time when initiating movement. Therefore, the lengthened decay time makes sense in the 19°C acclimated animals, and is expected.

t_{shift} probably corresponds largely to the nerve conduction velocity at different temperatures, which seems to increase with acute temperature. While the effect on t_{shift} between acclimation groups was significant, it was only significant for 31°C. This effect may be explained by inconsistent Vaseline well placement for stimulating the nerve. If the well were placed farther towards the extremities of the nerve, the conduction time

would be longer. If this were consistently done in the 19°C acclimated animals, it could explain the significant result here.

In terms of the testing error, looking at Figures 8 and 9, the fits are visually good. The reported error, however, is quite high in some cases. The chosen error metric calculates the error at all sample points. As a comparison, Sen et al. (1996) chose to calculate error based on EJP peak height only. Because the baseline was inherently noisy, and there are more sample points than there are EJP peaks, the overall error calculated using all sample points will necessarily be worse than if only the peaks were compared. There is also a certain amount of interanimal variability in the results. For example, the standard deviation of the test error was 14.2%. This variability must also have contributed to the level of the errors.

The fact that significant differences are not seen across the board between acclimation temperatures and rather, are specific to particular acute temperatures is likely an effect of having a very limited dataset. In fact, many of the tests for statistical significance were below the suggested power level (0.8) because of insufficient sample size. If the size of the data pool were increased I postulate that several things may happen. I would expect to see a decrease in the maximum amplitude of the EJPs as a function of not only increasing acute but also warmer acclimation temperature. As my data above show, the 7°C EJPs were significantly larger in amplitude than their 19°C counterparts in the 7°C acute case. I expect that further experiments might yield significant differences in EJP amplitude between acclimation groups across all acute temperatures. With reference to the EJP decay time constant, τ_1 , I would expect further

experiments to yield significantly longer EJP decay times in 19°C animals at the higher temperatures as well as those which were found to be significant here.

It is unfortunate that I was unable to analyze the higher temperature data because of the multiple responses. If the stimulus times were able to be accurately extracted and used to train the model, I would expect that the net facilitation (either K_2 or F) would get higher with acute temperature. This is corroborated by Figure 15. While it seems that perhaps the facilitation between the acclimation groups would vary at that extreme, it is unclear that it would before that point. These multiple spikes may be another form of compensation for long term exposure to high temperatures – by single spikes causing multiple spikes in the motor axons, the crab would have more activation of muscles at higher temperatures which could compensate for the shorter EJP time course and the smaller amplitude.

Acknowledgements / Epilogue

Everyone in the lab has helped me out at one point or another – small questions / clarifications and even just being around to chat with. So thanks, everybody.

Thank you Eve, firstly, for letting me do this work in your lab, and secondly for always being available to talk and answer questions. Every time I went into your office with something that was worrying me, I left feeling like everything would be OK, and so far, at least, you have always been right.

I could not have done most of this without the help of two people in particular – Lamont Tang and Adam Taylor. Lamont was the person who initially suggested me talking with Eve to see if I could do some work here. He also helped me a lot with getting my preps to cooperate with me on the rig. Adam helped me a great deal with the modeling and analysis of the models, and he gave me a crash course in Matlab, which has proved to be extremely ~~useful~~ necessary. Like I said, without either of you, this would not have been possible, so I owe each of you something (though I'm not quite sure what).

I'd like to thank Nelson Cruz-Bermúdez for initially showing me how to do the dissection of the gm6 which led me to doing this.

Thanks to Mehmet for offering good advice and laughing in the face of danger.

Doing these experiments has not been easy. In fact, this has been pretty much the hardest thing I've ever attempted. But I think it was worth it. I got to do things that very few people get an opportunity to do, and for that I'm grateful. There is a lot of cool stuff to learn and to do, and I'm glad I got to see what learning is like from where learning and discovery is actually done – in the lab, not just in books.

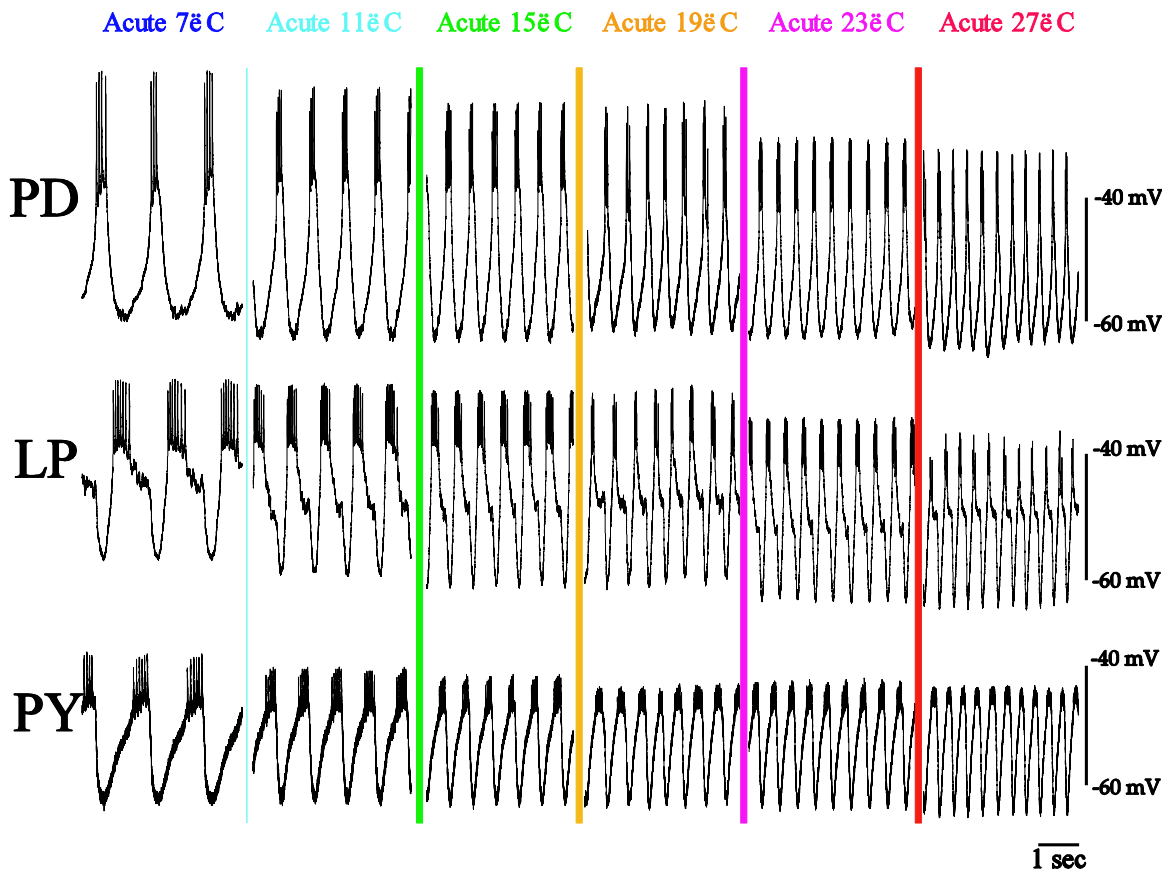
The end.

References

- CAMACHO, J., S. A. QADRI, H. WANG and M. K. WORDEN, 2006 Temperature acclimation alters cardiac performance in the lobster *Homarus americanus*. *J Comp Physiol A Neuroethol Sens Neural Behav Physiol* **192**: 1327-1334.
- DAYAN, P., and L. F. ABBOTT, 2001 *Theoretical Neuroscience*. The MIT Press, Cambridge, MA.
- HOOPER, S. L., M. B. O'NEIL, R. WAGNER, J. EWER, J. GOLOWASCH and E. MARDER, 1986 The innervation of the pyloric region of the crab, *Cancer borealis*: homologous muscles in decapod species are differently innervated. *J Comp Physiol [A]* **159**: 227-240.
- JORGE-RIVERA, J. C., K. SEN, J. T. BIRMINGHAM, L. F. ABBOTT and E. MARDER, 1998 Temporal dynamics of convergent modulation at a crustacean neuromuscular junction. *J Neurophysiol* **80**: 2559-2570.
- KERKUT, G. A., and R. M. RIDGE, 1961 The effect of temperature changes on the resting potential of crab, insect and frog muscle. *Comp Biochem Physiol* **3**: 64-70.
- LAZARUS, R. E., P. J. STEPHENS and N. MINDREBO, 1982 The peripheral generation of action potentials in excitatory motor neurons of a crab. *J Exp Zool* **222**: 129-136.
- LENZ, P. H., A. E. HOWER and D. K. HARTLINE, 2005 Temperature compensation in the escape response of a marine copepod, *Calanus finmarchicus* (Crustacea). *Biol Bull* **209**: 75-85.
- MAYNARD, D. M., and M. R. DANDO, 1974 The structure of the stomatogastric neuromuscular system in *Callinectes sapidus*, *Homarus americanus* and *Panulirus argus* (Decapoda Crustacea). *Philos Trans R Soc Lond B Biol Sci* **268**: 161-220.
- SEN, K., J. C. JORGE-RIVERA, E. MARDER and L. F. ABBOTT, 1996 Decoding synapses. *J Neurosci* **16**: 6307-6318.
- STEPHENS, P. J., 1985 Temperature effects on a slow-crustacean neuromuscular system. *Comp Biochem Physiol A* **82**: 591-595.
- STEPHENS, P. J., and H. L. ATWOOD, 1981 Peripheral Generation and Modulation of Crustacean Motor Axon Activity at High Temperatures. *J Comp Physiol A Neuroethol Sens Neural Behav Physiol* **142**: 309-314.
- STEPHENS, P. J., and H. L. ATWOOD, 1982 Thermal acclimation in a crustacean neuromuscular system. *J Exp Biol* **98**: 39-47.
- STEPHENS, P. J., and R. E. LAZARUS, 1981 Ethanol and temperature modify motor axon firing patterns. *Brain Res* **229**: 260-263.
- WORDEN, M. K., C. M. CLARK, M. CONAWAY and S. A. QADRI, 2006 Temperature dependence of cardiac performance in the lobster *Homarus americanus*. *J Exp Biol* **209**: 1024-1034.

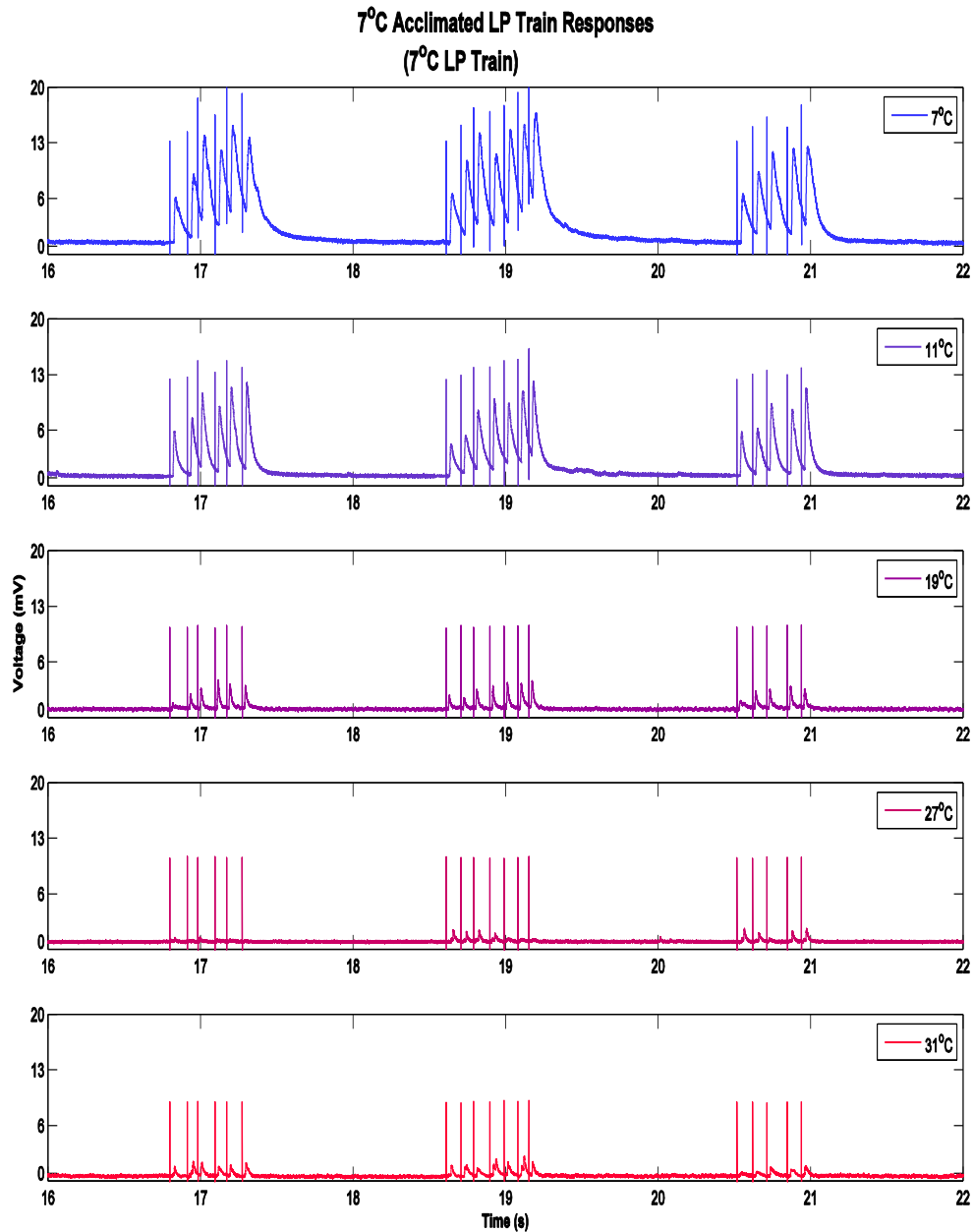
Figures:

Figure 1 – Network Activity as a Function of Acute Temperature



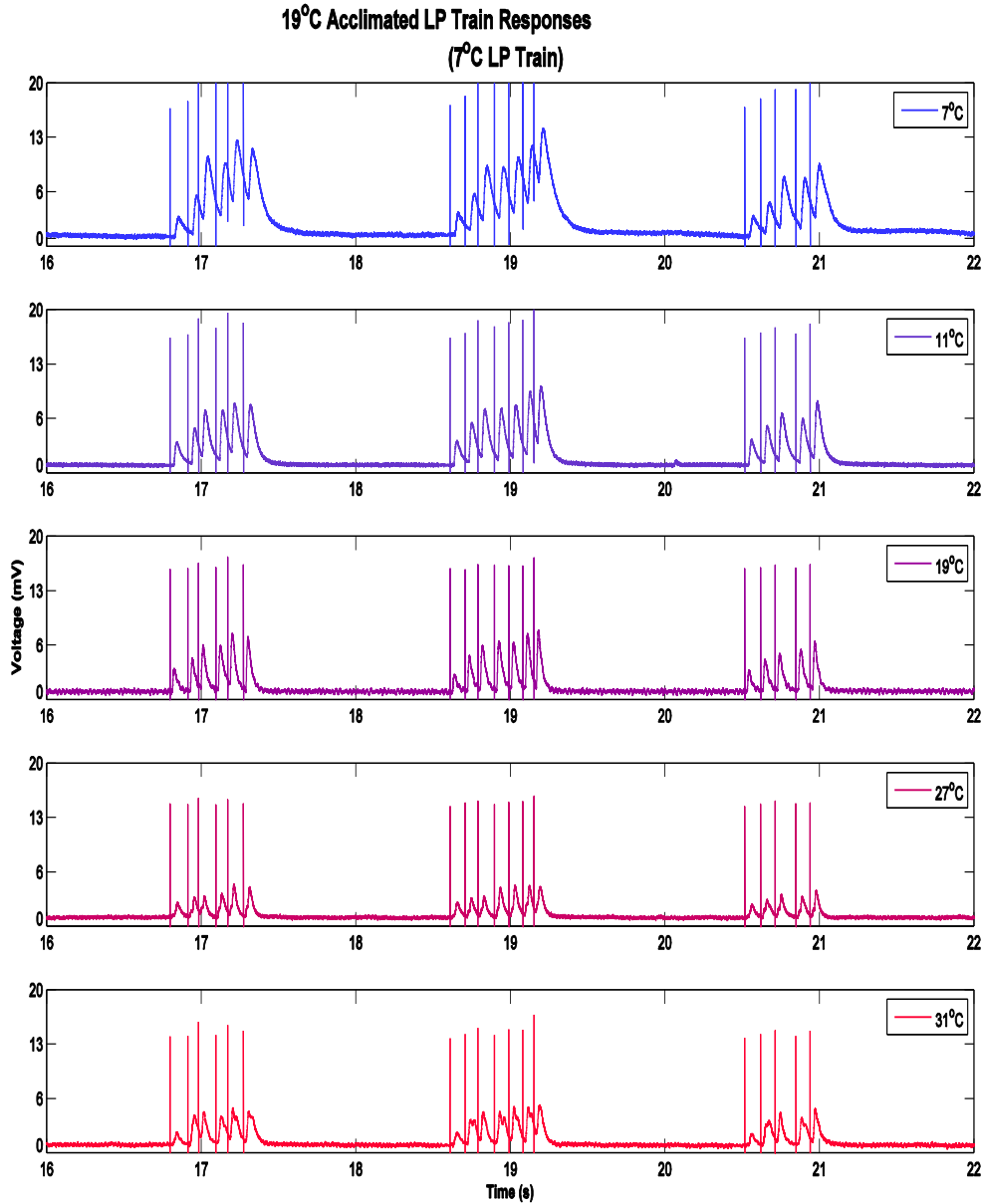
Plots of the Pyloric Dilator (PD), Lateral Pyloric (LP), and Pyloric (PY) neurons at varying acute temperatures - the slow wave frequency increases as acute temperature rises (courtesy of Tang et al.).

Figure 2 – LP Stimulus Responses Across Temperature in a 7°C Acclimated Animal



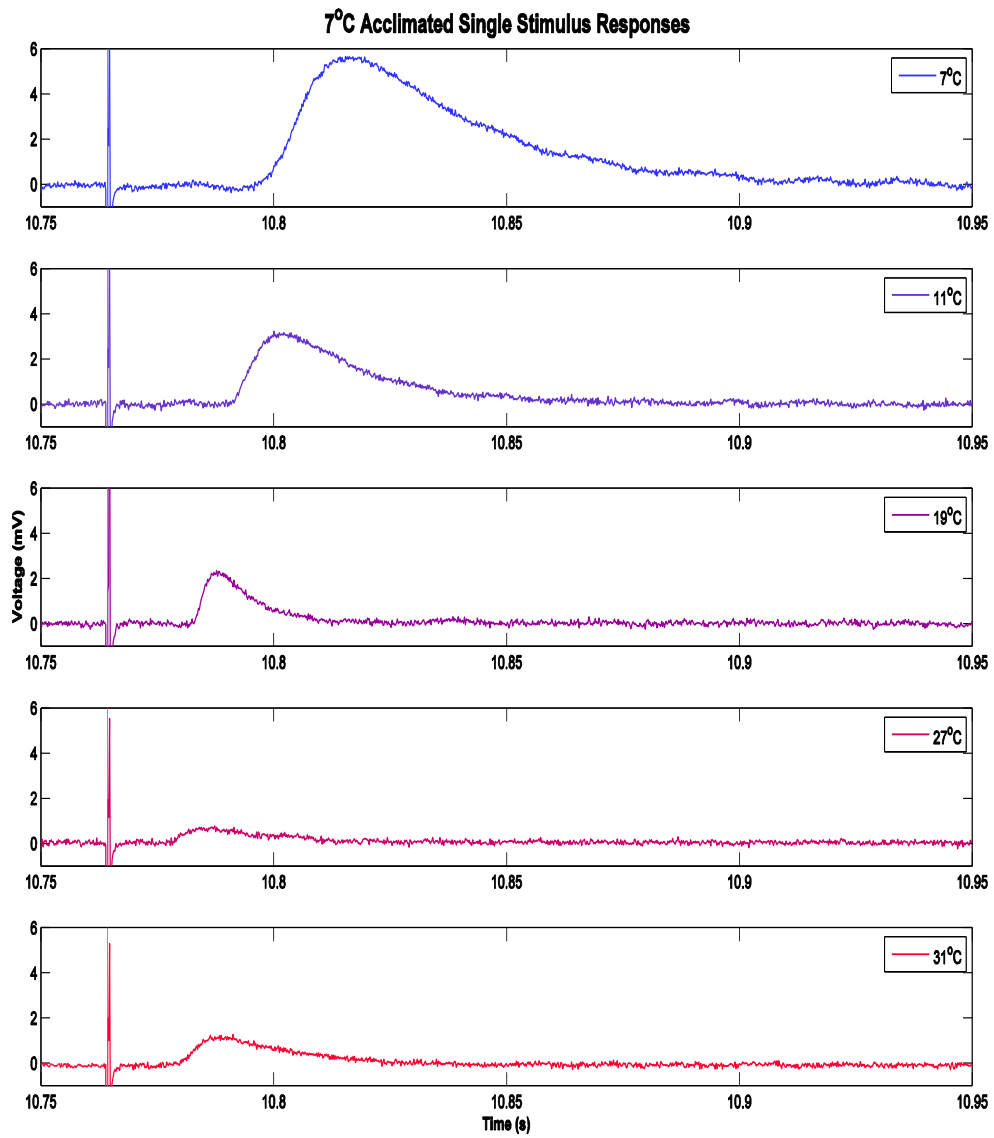
Raw traces from the P1 muscle response when given a single LP train at varying acute temperatures in an animal acclimated to 7°C. The stimulus train was recorded from the LP neuron at an acute temperature of 7°C. Maximum amplitude notably decreases with temperature. These traces were used to assess the accuracy of the model after fitting. Resting membrane potential was subtracted from the trace to set a baseline of zero. Large spikes are stimulus artifacts.

Figure 3 – LP Stimulus Responses Across Temperature in a 19°C Acclimated Animal



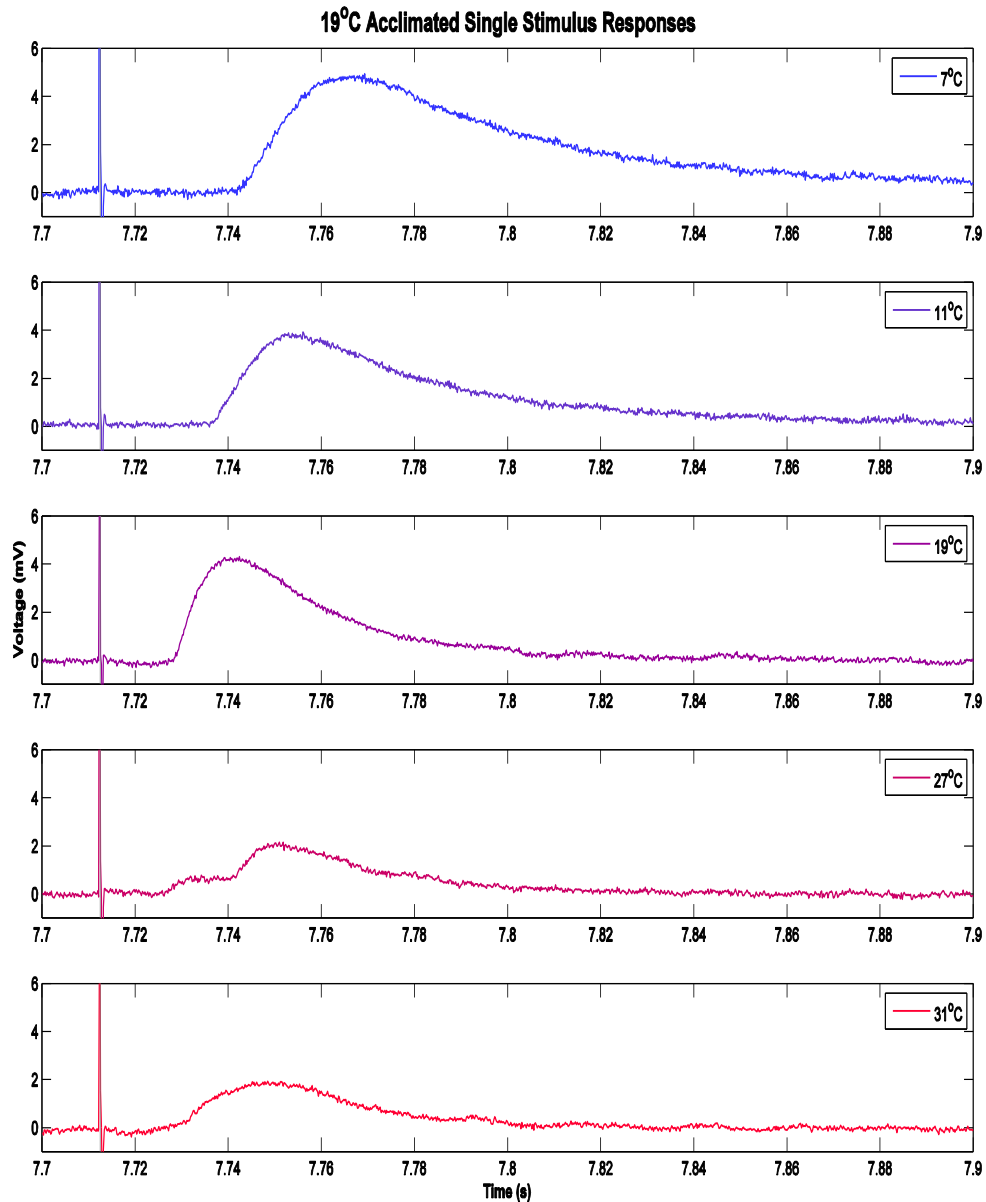
Similar to Figure 2, each plot shows a raw trace from the P1 muscle response when given a single LP train at varying acute temperatures in an animal acclimated to 19°C. As with 7°C acclimated animals, maximum amplitude notably decreases with temperature. These traces were used to assess the accuracy of the model after fitting. Resting membrane potential was subtracted from the trace to set a baseline of zero. Large spikes are stimulus artifacts.

Figure 4 – Single Stimulus Responses at Varying Acute Temperature in a 7°C Acclimated Animal



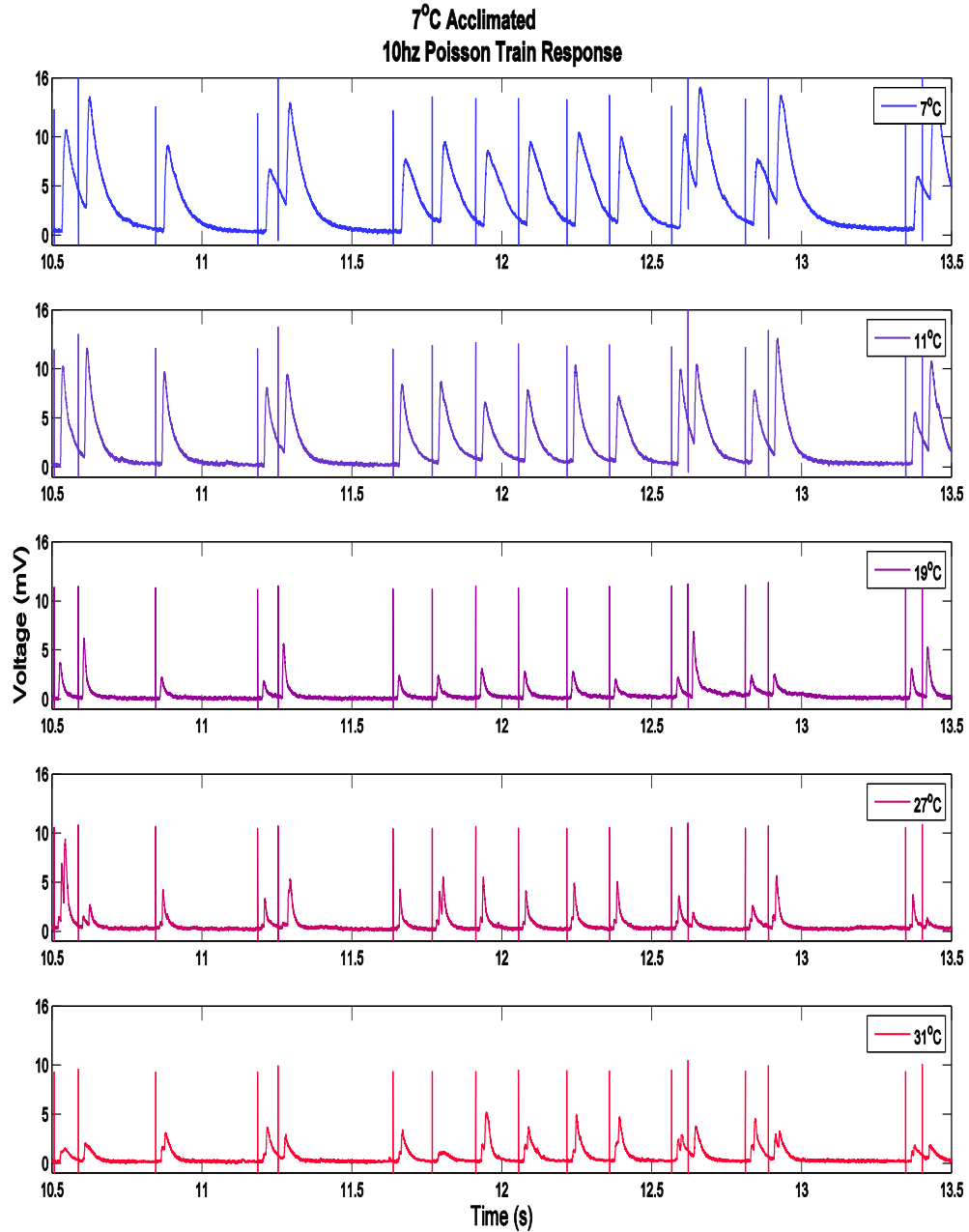
Raw traces from a slow (1Hz) Poisson stimulus train used to characterize single EJP characteristics in an animal acclimated to 7°C at varying acute temperature. Maximum EJP amplitude visibly varies with temperature as does the time from stimulus to threshold. Resting membrane potential was subtracted from the trace to set a baseline of zero. (Recorded from the same animal as Figure 2.)

Figure 5 – Single Stimulus Responses at Varying Acute Temperature in a 19°C Acclimated Animal



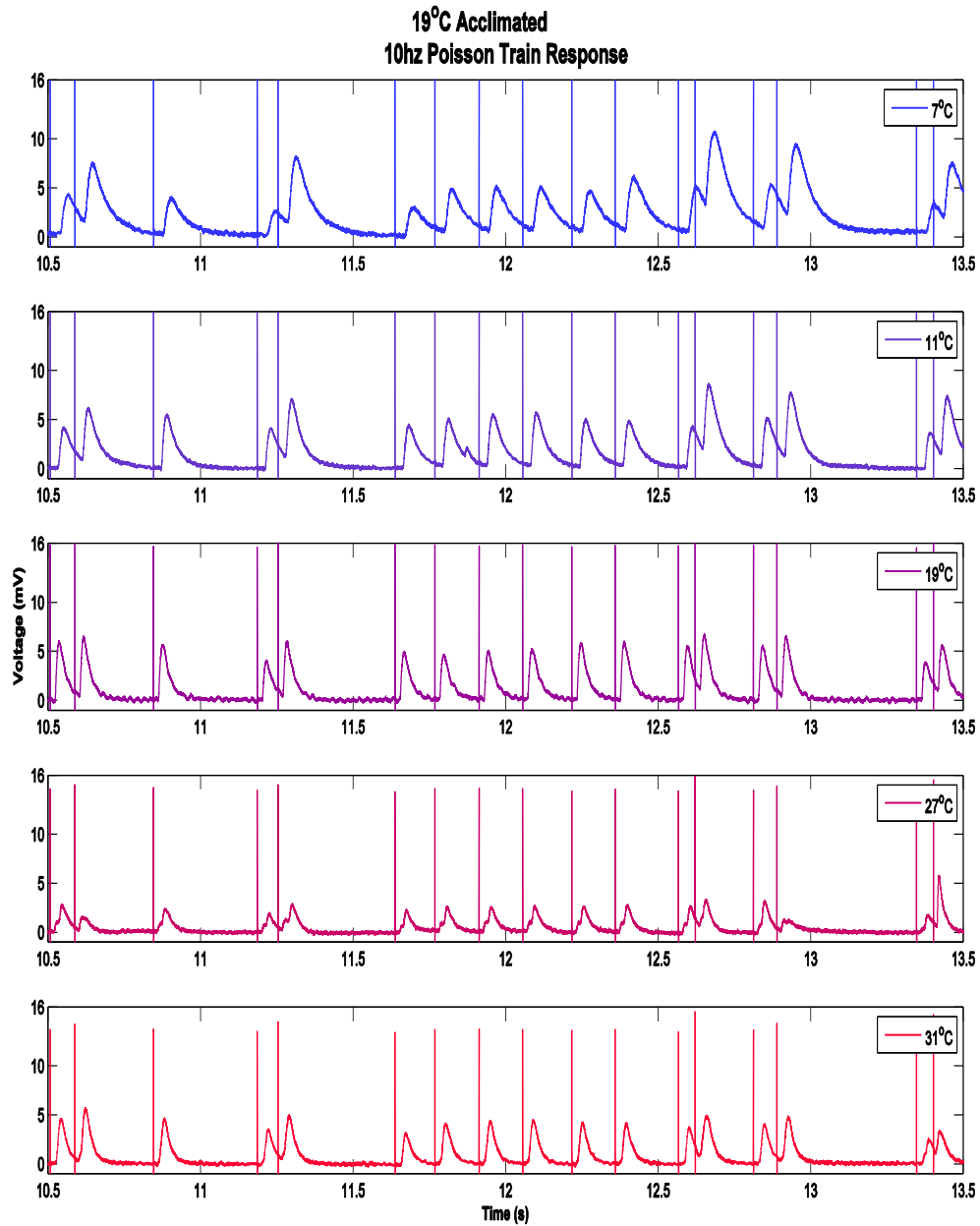
Similar to Figure 4, this shows raw traces from a slow (1Hz) Poisson stimulus train used to characterize single EJP characteristics in an animal acclimated to 7°C at varying acute temperature. Again, maximum EJP amplitude visibly varies with temperature as does the time from stimulus to threshold. Resting membrane potential was subtracted from the trace to set a baseline of zero. (Recorded from the same animal as Figure 3.)

Figure 6 – 10Hz Poisson Train Responses at Varying Acute Temperature in a 7°C Acclimated Animal



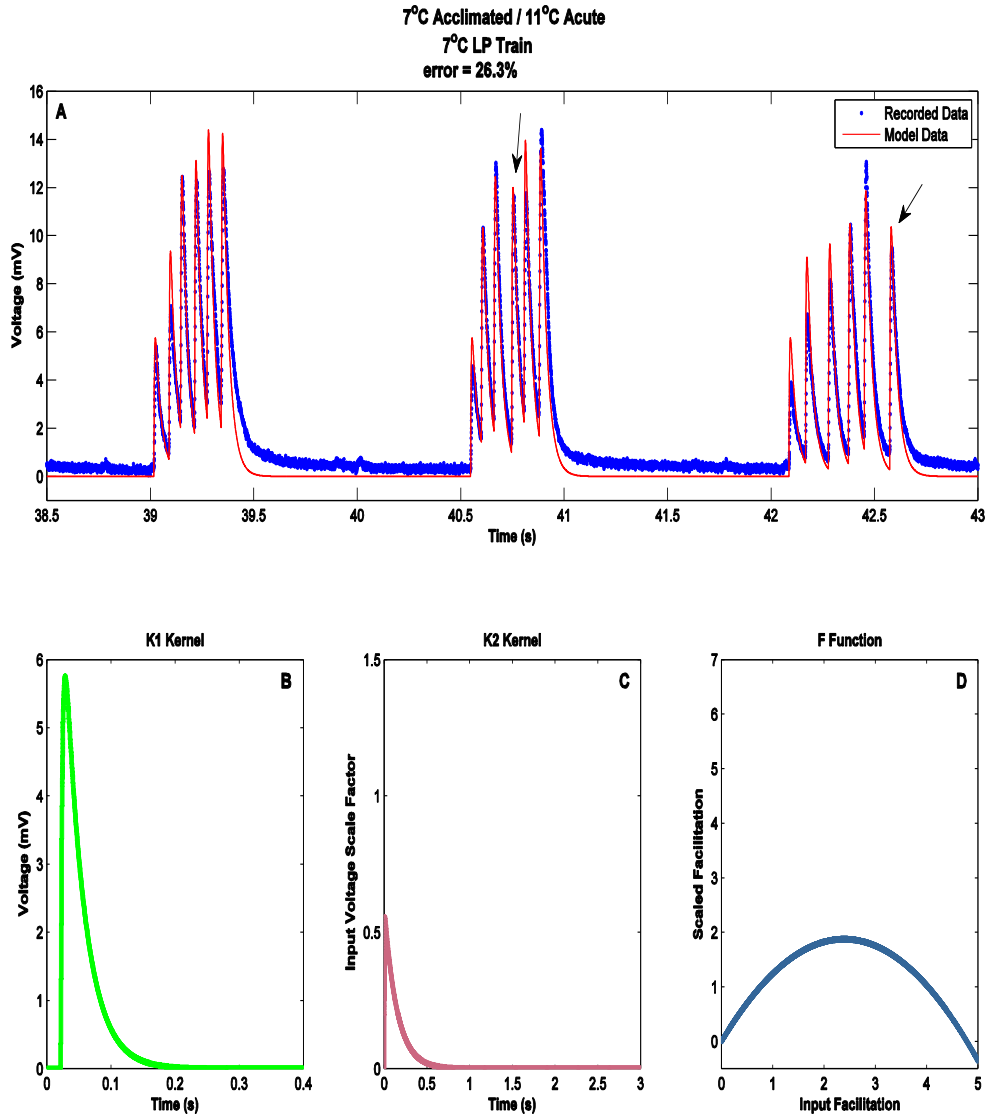
Excerpts from a 10Hz Poisson train delivered to the muscle of an animal acclimated to 7°C at varying acute temperature. These stimulus trains served as data on which to train the model. Vertical lines represent stimulus artifacts. Resting membrane potential was subtracted from the trace to set a baseline of zero. (Recorded from the same animal as in Figures 2 and 4.) (Other Poisson trains described in materials and methods.)

Figure 7 – 10Hz Poisson Train Responses at Varying Acute Temperature in a 19°C Acclimated Animal



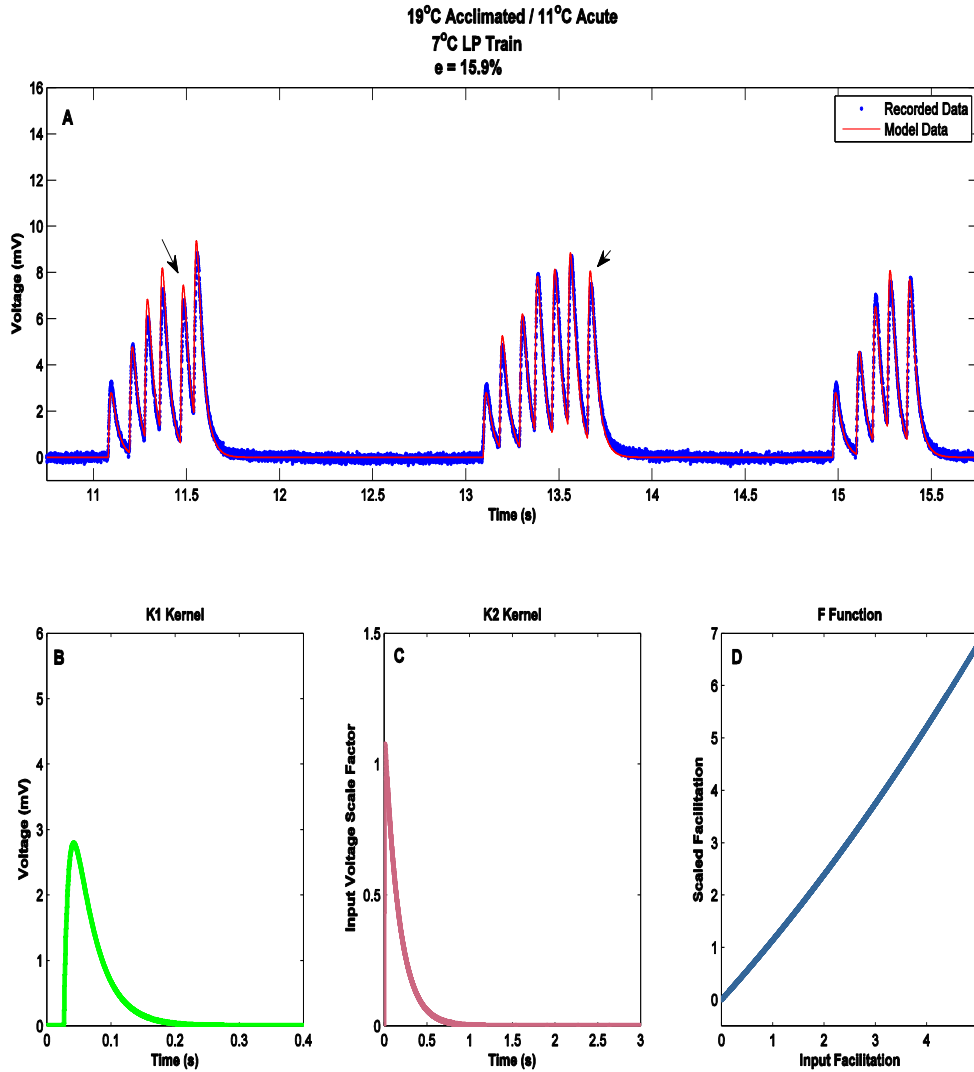
Excerpts from a 10Hz Poisson train delivered to the muscle of an animal acclimated to 19°C at varying acute temperature. These stimulus trains served as data on which to train the model. Vertical lines represent stimulus artifacts. Resting membrane potential was subtracted from the trace to set a baseline of zero. (Recorded from the same animal as in Figures 3 and 5.) (Other Poisson trains described in materials and methods.)

Figure 8 – Raw Data and Model Fit at 11°C Acute Temperature in a 7°C Acclimated Animal



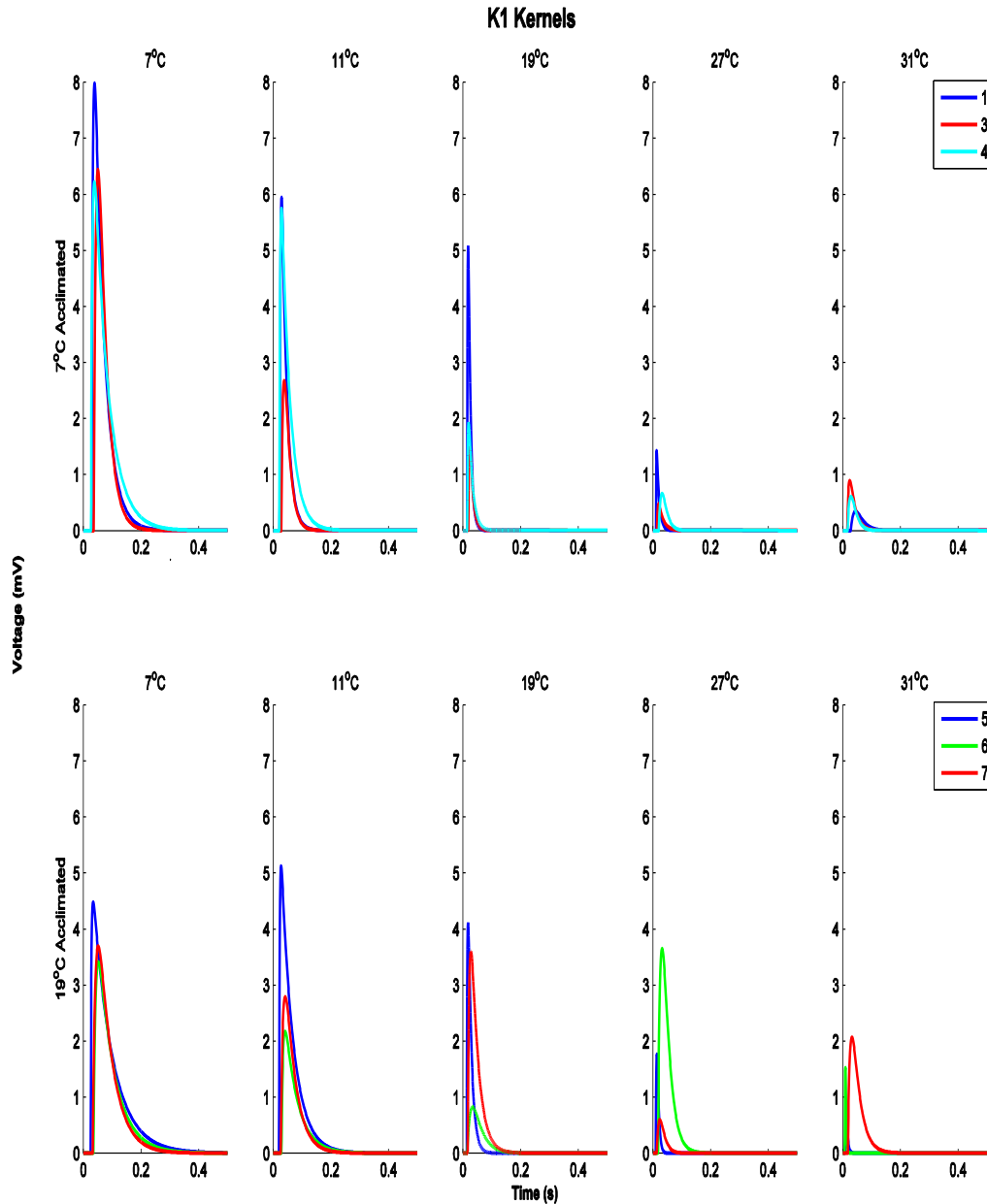
A. Recording of the response in an animal acclimated to 7°C when given an LP train at 11°C acute temperature (blue). Expected response of the P1 muscle from an animal acclimated to 7°C at 11°C acute temperature, given the final parameters of the model for this particular animal at this acute temperature (red). Error reported is relative RMS error (for explanation see materials and methods). Despite the seemingly high error, the model correctly predicts subtleties in overall muscle response, such as depression in the middle and at the end of an LP burst (arrows). *B.* Final fit of the K1 kernel for this animal at 11°C. *C.* Final fit of the K2 kernel (facilitation kernel) for this animal at 11°C. *D.* Final fit of the F function (facilitation scale function) for this animal at 11°C. (Recorded from the same animal as in Figures 2, 4, and 6) (LP train recorded at an acute temperature of 7°C. Resting membrane potential was subtracted from the trace to set a baseline of zero. Stimulus artifacts were removed – see materials and methods).

Figure 9 – Raw Data and Model Fit at 11°C Acute Temperature in a 19°C Acclimated Animal



A. Recording of the response in an animal acclimated to 19°C when given an LP train at 11°C acute temperature (blue). Expected response of the P1 muscle from an animal acclimated to 19°C at 11°C acute temperature, given the final parameters of the model for this particular animal at this acute temperature (red). Error reported is relative RMS error (see materials and methods for explanation). This error is less than that of the shown 7°C acclimated animal in Figure 8, and again the model correctly predicts subtleties in overall muscle response, such as rapid depression in the middle and the end of an LP burst (arrows). *B.* Final fit of the K1 kernel for this animal at 11°C. *C.* Final fit of the K2 kernel (facilitation kernel) for this animal at 11°C. *D.* Final fit of the F function (facilitation scale function) for this animal at 11°C. (Recorded from the same animal as in Figures 2, 4, and 6) (LP train recorded at an acute temperature of 7°C. Resting membrane potential was subtracted from the trace to set a baseline of zero. Stimulus artifacts were removed – see materials and methods).

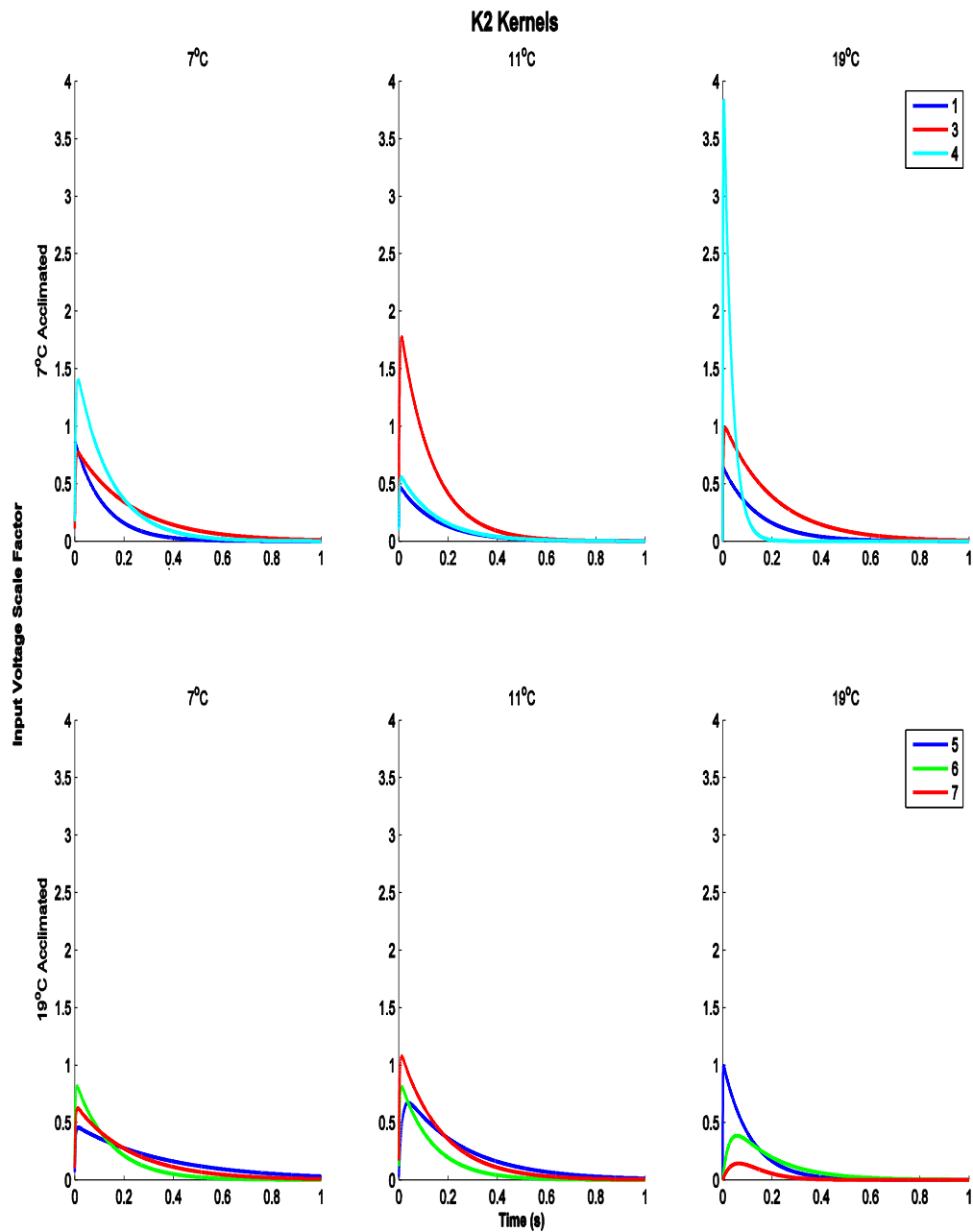
Figure 10 – Final Fits of K1 Kernels



Final fits for the K1 kernel for all animals. Top panel: K1 kernels from 7oC acclimated animals at increasing acute temperature. Bottom panel: K1 kernels from 19oC acclimated animals at increasing acute temperature. Models were created for each animal in both acclimation groups at every acute temperature (30 total). With increasing acute temperature, an apparent decrease in K1 maximum amplitude is observed. Additionally, the time course seems to decrease (speed up).

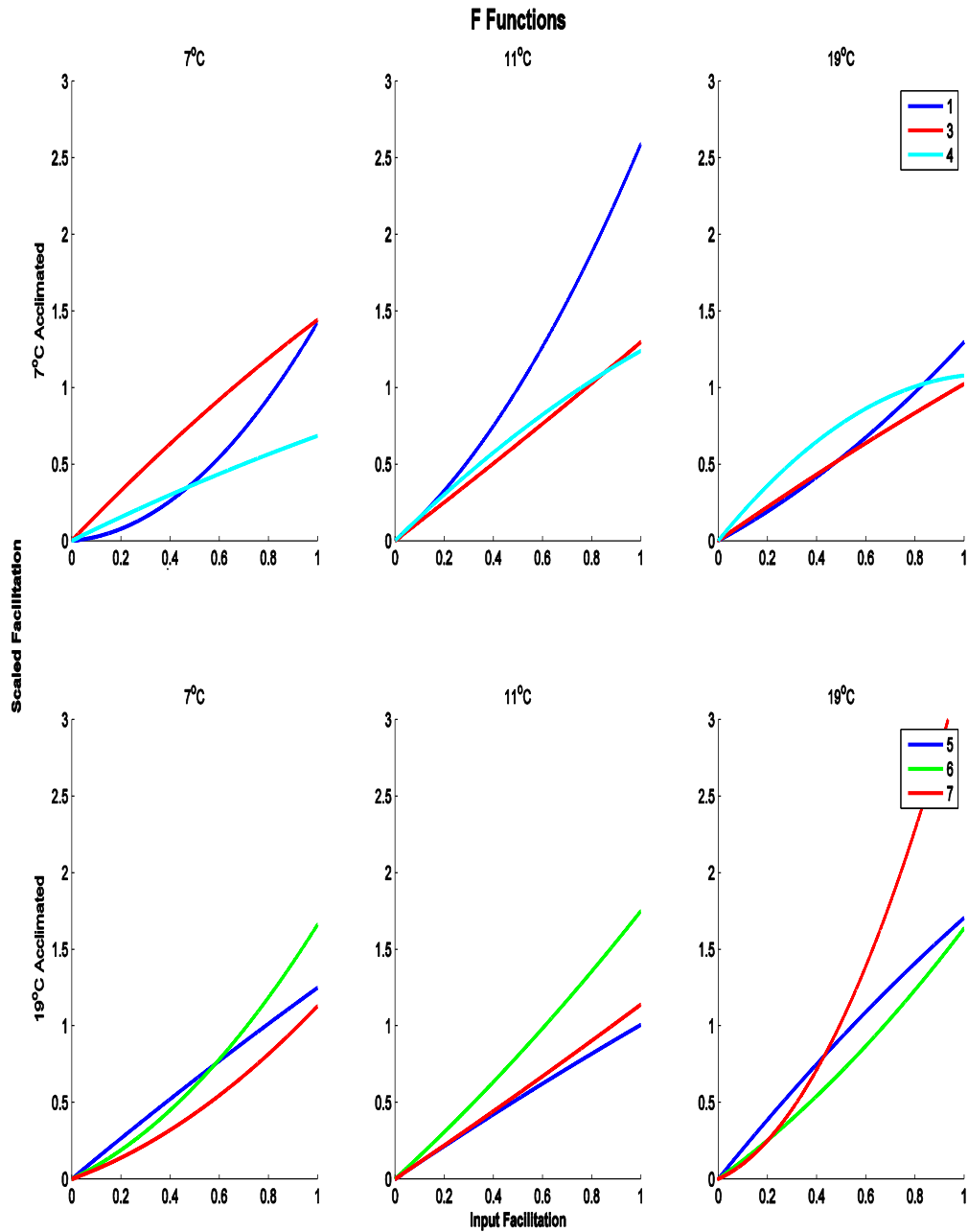
[Animals 2 (7°C Acclimated) and 8 (19°C Acclimated) showed abnormal responses and were not included in the analysis. (Animal 4 – 7oC, from Figures 2,4,6,8; Animal 7 – 19oC - from Figures 3,5,7,9).]

Figure 11 – Final Fits of K2 Kernels



Final fits for the K2 kernel for all animals. Top panel: K2 kernels from 7°C acclimated animal models at increasing acute temperature. Bottom panel: K2 kernels from 19°C acclimated animal models at increasing acute temperature. Models were created for each animal in both acclimation groups at every acute temperature (30 total). Unexpected experimental results impeded analysis at acute temperatures above 19°C (see text). [Animals 2 (7°C Acclimated) and 8 (19°C Acclimated) showed abnormal responses and were not included in the analysis. (Animal 4 – 7°C, from Figures 2,4,6,8; Animal 7 – 19°C - from Figures 3,5,7,9).]

Figure 12 – Final Fits of F Functions



Final fits for the F functions for all animals. Top panel: F functions from 7°C acclimated animal models at increasing acute temperature. Bottom panel: F functions from 19°C acclimated animal models at increasing acute temperature. Models were created for each animal in both acclimation groups at every acute temperature (30 total). Unexpected experimental results impeded analysis at acute temperatures above 19°C (see text). [Animals 2 (7°C Acclimated) and 8 (19°C Acclimated) showed abnormal responses and were not included in the analysis. (Animal 4 – 7oC, from Figures 2,4,6,8; Animal 7 – 19oC - from Figures 3,5,7,9).]

Figure 13 – K1 Final Parameters

Parameters for all animals at each temperature after fitting the model to the data. Models were created for each animal in both acclimation groups at every acute temperature (30 total).

A. V_{max} – the maximum amplitude of the K1 kernel. Top graph – V_{max} parameters of 7°C acclimated animal models at increasing acute temperatures. Bottom graph – V_{max} parameters of 19°C acclimated animal models at increasing acute temperatures. Acute temperature had a significant effect on V_{max} in 7°C acclimated animals ($P < 0.005$, ♥♣Δ♠♦). A significant effect was also found within the 7°C acute model parameters between acclimation groups ($P < 0.05$, ψ).

B. τ_{1} – the falling time constant of the K1 kernel. Top graph – τ_{1} parameters of 7°C acclimated animal models at increasing acute temperatures. Bottom graph – τ_{1} parameters of 19°C acclimated animal models at increasing acute temperatures. Acute temperature had a significant effect on τ_{1} in both the 7°C acclimated animals ($P < 0.005$, Ø*), and within the 19°C acclimated animals ($P < 0.001$, ♥♣Δ♠♦). Acclimation temperature had a significant effect on τ_{1} at acute temperatures of 7°C and 11°C ($P < 0.05$, $\psi+$).

C. t_{shift} – time from stimulus to threshold of the K1 kernel. Top graph – t_{shift} parameters of 7°C acclimated animal models at increasing acute temperatures. Bottom graph – t_{shift} parameters of 19°C acclimated animal models at increasing acute temperatures. Acute temperature had a significant effect on t_{shift} in both the 7°C acclimated animals ($P < 0.005$, Ø*), and within the 19°C acclimated animals ($P < 0.01$, ♥♣Δ♠♦). A significant effect of acclimation temperature was found on the 31°C acute model parameters ($P < 0.05$, x).

D. Time to Peak – the time from threshold to V_{max} of the K1 kernel. Top graph – time to peak of 7°C acclimated animal models at increasing acute temperatures. Bottom graph – time to peak of 19°C acclimated animal models at increasing acute temperatures. While time to peak is not a strict parameter of the model, it is determined by τ_{1} and τ_{2} (see equation 7), and is more easily understood than τ_{2} .

[Animals 2 (7°C Acclimated) and 8 (19°C Acclimated) showed abnormal responses and were not included in the analysis. (Animal 4 – 7oC, from Figures 2,4,6,8; Animal 7 – 19oC - from Figures 3,5,7,9).]

Figure 13 - K1 Final Parameters:

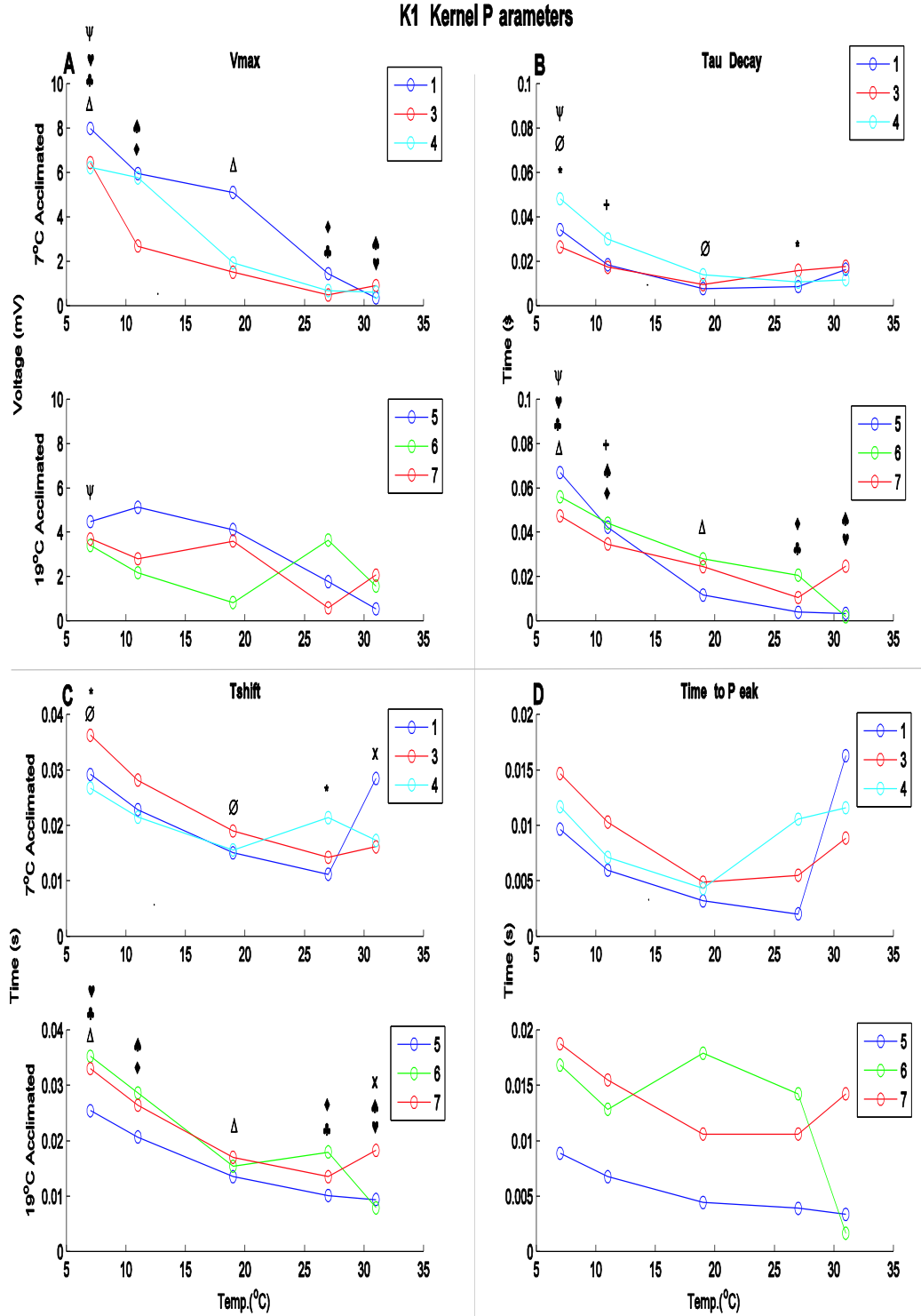
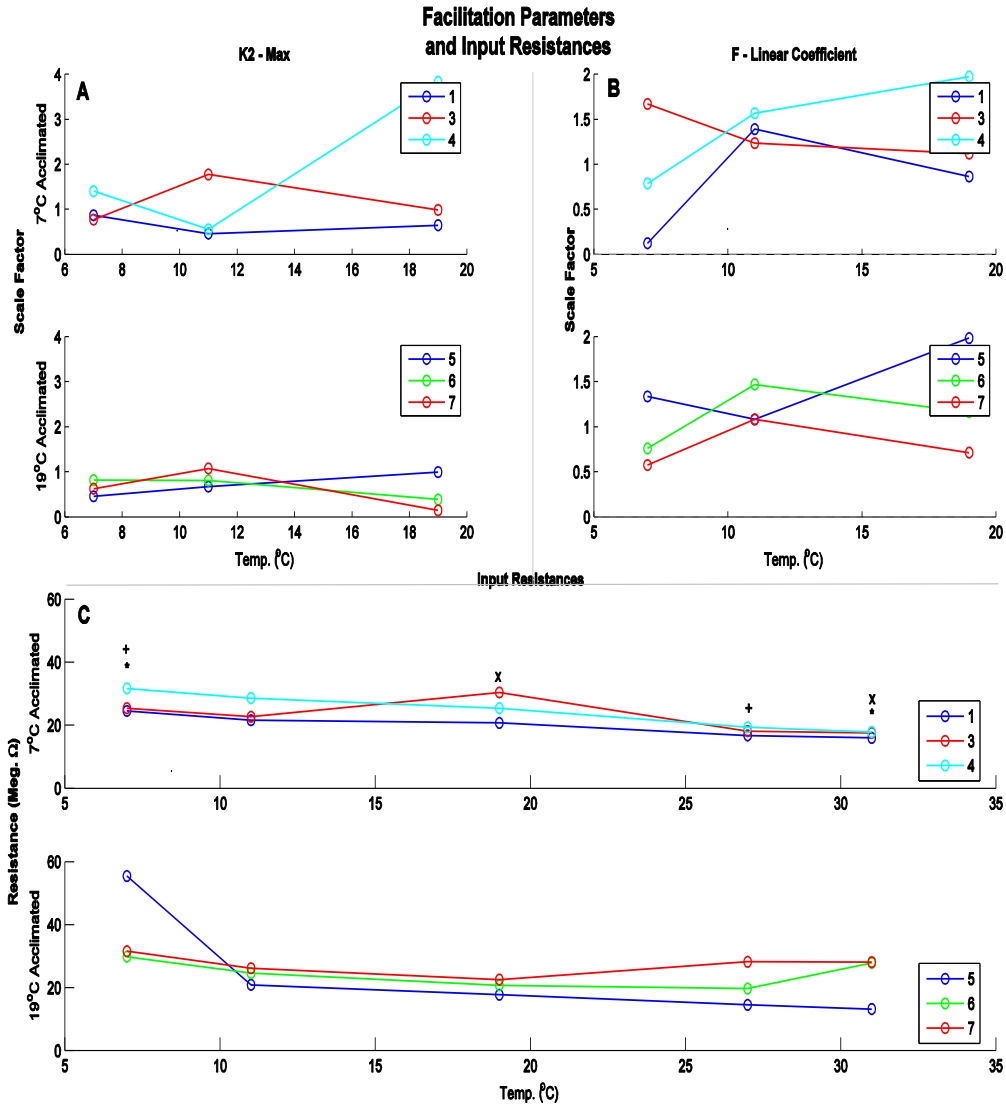


Figure 14 – Facilitation Parameters and Input Resistance

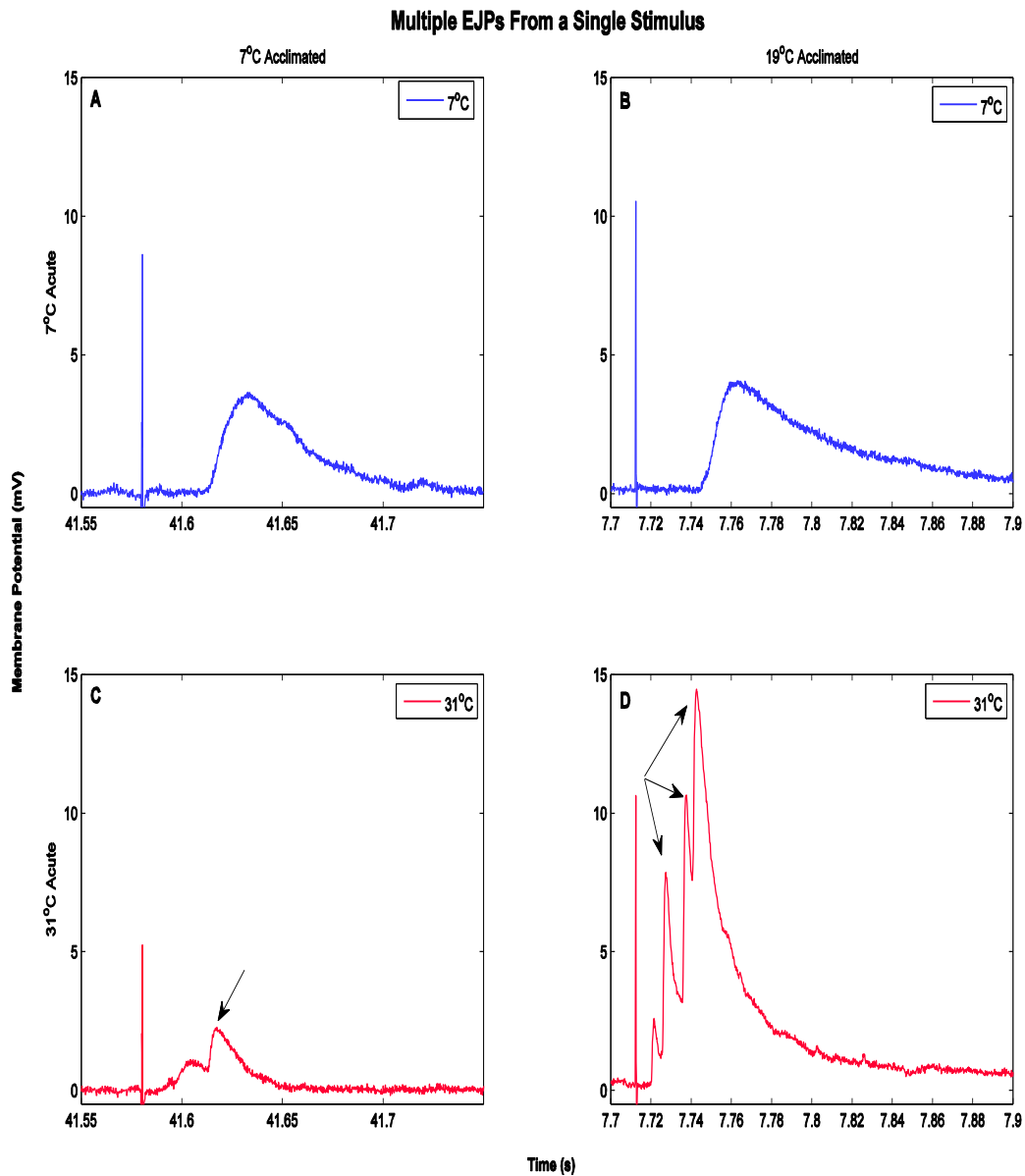


A. Max – maximum height of the K2 kernel. Top graph – *max* parameters of 7°C acclimated animal models at increasing acute temperatures. Bottom graph – *max* parameters of 19°C acclimated animal models at increasing acute temperatures.

B. Linear coefficient, *B*, of the F function. Top graph – *B* parameters of 7°C acclimated animal models at increasing acute temperatures. Bottom graph – *B* parameters of 19°C acclimated animal models at increasing acute temperatures.

C. Input Resistances of each animal at each acute temperature. Top graph – input resistance of 7°C acclimated animal muscle fibers at increasing acute temperatures. Bottom graph – input resistance of 19°C acclimated muscle fibers at increasing acute temperatures. Significant effects of acute temperature were found only in the 7°C acclimated animals ($P < 0.005$, *+x).

Figure 15 – Multiple EJPs from a Single Stimulus in Both Acclimation Temperatures



- A.* Response to a single stimulus in a 7°C acclimated crab at 7°C acute temperature.
- B.* Response to a single stimulus in a 19°C acclimated crab at 7°C acute temperature.
- C.* Response to a single stimulus in a 7°C acclimated crab at 31°C acute temperature. A second EJP occurs just after the first starts to decay.
- D.* Response to a single stimulus in a 19°C acclimated crab at 31°C acute temperature. Three additional EJPs are elicited after the first expected response. The maximum amplitude of the total response is higher than at 7°C because of facilitation of the multiple EJPs.